Cancer Letters 454 (2019) 204–214

Contents lists available at ScienceDirect

Cancer Letters

journal homepage: www.elsevier.com/locate/canlet

Original Articles

Disruption of oncogenic liver-intestine cadherin (CDH17) drives apoptotic pancreatic cancer death

Xinjian Liu[a,b,c,1], Yue Huang[a,1], Hao Yuan[a,b,d], Xiaoqiang Qi[a,b], Yariswamy Manjunath[a,b], Diego Avella[a,b], Jussuf T. Kaifi[a,b], Yi Miao[d], Min Li[e], Kuirong Jiang[a,b,d,**], Guangfu Li[a,b,f,*]

[a] Department of Surgery, University of Missouri-Columbia, Columbia, MO, 65212, USA
[b] Ellis Fischel Cancer Center, University of Missouri-Columbia, Columbia, MO, 65212, USA
[c] Department of Pathogen Biology, Nanjing Medical University, Nanjing, Jiangsu, 211166, China
[d] Pancreas Center, The First Affiliated Hospital of Nanjing Medical University, Nanjing, Jiangsu, 210029, China
[e] Department of Medicine, The University of Oklahoma Health Sciences Center, Oklahoma City, OK, 73104, USA
[f] Molecular Microbiology and Immunology, University of Missouri-Columbia, Columbia, MO, 65212, USA

ARTICLE INFO

Keywords:
Cadherin-17 (CDH17)
Oncogene
Tumorigenesis
Panc02-H7 cells
siRNA
shRNA
CRISPR

ABSTRACT

Liver–intestine cadherin (CDH17) has been known to function as a tumor stimulator and diagnostic marker for almost two decades. However, its function in highly malignant pancreatic cancer (PC) has yet to be elucidated. Using different strategies including siRNA, shRNA, and CRISPR technology, we successfully induced knockdown and knockout of CDH17 in Panc02-H7 cells and established the corresponding stable cell lines. With these cells, we demonstrated that loss of CDH17 function not only suppressed Panc02-H7 cell growth *in vitro* but also significantly slowed orthotopic tumor growth *in vivo, resulting in* the significant life extension. *In vitro* studies demonstrated that impairing CDH17 inhibited cell proliferation, colony formation, and motility by mechanistically modulating pro- and anti-apoptosis events in PC cells, as CDH17 suppression obviously increased expression of Bad, cytochrome C, cleaved caspase 3, and cleaved PARP, and reduced expression of Bcl-2, Survivin, and pAkt. *In vivo* studies showed CDH17 knockout resulted in apoptotic PC tumor death through activating caspase-3 activity. Taken together, CDH17 functions as an oncogenic molecule critical to PC growth by regulating tumor apoptosis signaling pathways and CDH17 could be targeted to develop an anti-PC therapeutic approach.

1. Introduction

Pancreatic cancer (PC) is the fourth-leading cause of cancer-related death accounting for about 3% of all cancers and about 7% of all cancer deaths [1,2]. The American Cancer Society estimates that in 2018, about 55,440 people will be diagnosed with PC and 44,330 will die of this disease; by 2030, PC will be the second-leading cause of cancer death in the US [3]. Worldwide, PC accounts for more than 200,000 deaths every year with an average 5-year survival rate of < 6% [4,5]. Surgical resection is possible only for a few early-stage patients (10–15%), but recurrence is common and the prognosis is very poor [6,7]. The lack of progress in prevention, early diagnosis, metastasis detection, and treatment underscores the need for increased efforts in PC research [8,9].

In 1994, liver–intestine cadherin, called cadherin-17 (CDH17) or human peptide transporter-1 (HPT-1), was characterized as a novel member of the cadherin superfamily. The cadherin superfamily is a type of cell adhesion molecules that play an important role in cell recognition, adhesion, and establishing cell-cell interaction [11,12]. Different from other members, an extracellular region of CDH17 contains seven cadherin domains [10]. As a component of the gastrointestinal tract, pancreatic CDH17 was shown to play a role in the morphological organization of liver and intestine. Disruption in expression or function of cadherins causes uncontrolled cell migration and proliferation during tumor development [13], therefore, CDH17 was also deemed to play a role in tumorigenesis and diagnosis [14]. In 2001, Grotzinger et al. first reported that CDH17 is a reliable and powerful marker molecule that can be used for early detection of gastric intestinal metaplasia and well-

* Corresponding author. Department of Surgery, Molecular Microbiology &Immunology, Ellis Fischel Cancer Center, University of Missouri-Columbia, One Hospital Dr., Medical Sciences Building, M272, Columbia, MO, 65212, USA.
** Corresponding author. Pancreas Center, The First Affiliated Hospital of Nanjing Medical University, 300 Guangzhou Road, Nanjing, Jiangsu, 210029, China.
E-mail addresses: jiangkuirong@njmu.edu.cn (K. Jiang), liguan@health.missouri.edu (G. Li).
[1] Xinjian Liu & Yue Huang contributed equally to this manuscript as first authors.

https://doi.org/10.1016/j.canlet.2019.04.022
Received 6 December 2018; Received in revised form 10 April 2019; Accepted 15 April 2019

differentiated adenocarcinomas [15]. Their clinically relevant studies with human tumor tissue validated the positive relationship between CDH17 expression and gastric cancer progression [16]. In 2014, Dr. Wang et al. demonstrated that CDH17 is able to induce tumorigenesis and lymphatic metastasis in gastric cancer by activating NF-κB signaling pathways [17]. In 2017, Li et al. reported that silencing CDH17 with siRNAs suppresses gastric cancer growth *in vitro* and *in vivo* [18]. In 2009, another group demonstrated that RNA interference-mediated knockdown of CDH17 inhibited proliferation of both primary and highly metastatic hepatocellular carcinoma (HCC) *in vitro* and *in vivo* [19]. These studies reveal the tumorigenic effect of CDH17 and its clinical value in cancer diagnosis and treatment.

Although CDH17 has been demonstrated to promote growth in gastric and liver cancer for almost two decades [15], the role and mechanisms of action of CDH17 in other cancers including PC have yet to be elucidated. Using approaches including siRNA, shRNA, or CRISPR technologies, we have successfully conducted knockdown and knockout of CDH17 in Panc02-H7 cells and established the corresponding stable cell lines. Using these cells and approaches, we performed the loss-of-function studies to comprehensively investigate the role of CDH17 disruption in modulating PC development and the underlying mechanisms. The results gained from our *in vitro* and *in vivo* experiments suggest that CDH17 functions as an oncogene, promoting PC development by modulating cell survival and apoptosis signaling pathways.

2. Materials and methods

2.1. Antibodies and plasmids

Antibodies against cleaved PARP, Akt, p-Akt (Thr308), Bcl-2, survivin, Bad, Bax, cytochrome C, cleaved caspase3, GAPDH, and Ki67 were purchased from Cell Signaling (Danvers, MA). Anti-mouse CDH17 antibody was purchased from R&D systems (Minneapolis, MN). Antibodies against human CDH17, β-actin, E-cadherin, N-cadherin, CDH16 were purchased from Abcam. All immunohistochemistry (IHC) reagents including ImmPRESS™ HRP anti-rabbit IgG (Peroxidase) (Cat#MP-7401), ImmPACT DAB peroxidase (HRP) substrate (Cat#SK-4105), and Hematoxylin (Cat#H-3404) were purchased from Vector Laboratories (Burlingame, CA).

LentiCas9-EGFP plasmid (Cat#63592) and pLL3.7 plasmid were purchased from Addgene (Cambridge, Massachusetts, USA), human and mouse CDH17 recombinant plasmids were purchased from OriGene (Rockville, MD).

2.2. Cell lines, medium, and culture

Mouse Panc02 cells were obtained from NIH. Panc02-H7 cells, an invasive cell line derived from Panc02 [20], were a generous gift from Dr. Keping Xie of MD Anderson Cancer Center. The cell line was maintained in Dulbecco's Modified Eagle Medium (DMEM; Cellgro, Manassas, VA) supplemented with 100 U/mL penicillin, 100 μg/mL streptomycin, 2 mmol/L L-glutamine, 10 mmol/L HEPES, and 10% fetal bovine serum (FBS) at 37 °C in a 5% CO_2 humidified atmosphere [21]. Human PC cell lines including Panc-1, MIA PaCa-2, and BxPC-3 were purchased from ATCC (Manassa, VA). Human Panc-1 and MIA PaCa-2 cells were cultured in DMEM supplemented with 10% FBS, 2.5% equine serum and 100 U/mL penicillin, 100 μg/mL streptomycin at 37 °C in 5% CO_2 humidified incubator. Human BxPC-3 cells were cultured in RPMI-1640 media supplemented with 10% FBS and 100 U/mL penicillin, 100 μg/mL streptomycin at 37 °C in 5% CO_2 humidified incubator.

2.3. Mice

Male C57BL/6 mice were purchased from Jackson Laboratory (Bar Harbor, ME). All experiments with mice were performed under a protocol approved by the University of Missouri Animal Care and Use Committee. All mice received humane care according to the criteria outlined in the “Guide for the Care and Use of Laboratory Animals”.

2.4. CDH17 siRNA transfection

To knock down CDH17 with siRNA, the mouse and human PC cells, grown to 50% confluence in 6-well plate, then received siRNA transfection with RNAi-MAX Lipofectamine reagent (Invitrogen, Carlsbad, CA). 5 pmol siRNAs were used to transfect mouse Panc02-H7 cells, 30 pmol siRNA were transfected human Panc-1 or MIA PaCa-2 cells. All the designed mouse or human CDH17-siRNAs or negative control (NC) siRNAs were purchased from IDT (Coralville, IA). Eight hours post-transfection, the medium was replaced with complete DMEM medium containing 10% fetal bovine serum (FBS). Cells were cultured for another 36 h for subsequent assays.

2.5. CDH17 recombinant plasmid transfection

To induce ectopic CDH17 expression in mouse and human PC cell lines, the cells were grown to 70% confluence in 6-well plate, then received transfection of 2.5 μg of mouse or human CDH17 recombinant plasmid (OriGene, Rockville, MD) with Lipofectamine 3000 reagent (Thermo Fisher Scientific, Waltham, MA). Eight hours post-transfection, the medium was replaced with complete DMEM medium containing 10% FBS. Cells were cultured for another 48 h for subsequent assays.

2.6. Using shRNA approach to establish stable CDH17 knockdown cells

To knockdown CDH17 with shRNA, CDH17-shRNAs were designed, synthesized, and annealed to form double chain DNA fragments which were cloned into vector pLL3.7 between *Hpa*I and *Xho*I sites [22]. The recombinant CDH17-shRNA plasmid or scrambled shRNA plasmid together with helper plasmids pMD2.G and psPAX2 were transfected into HEK293 cells to package the CDH17-shRNA-recombinant lentivirus. The packaged virus particles in culture supernatant were harvested and concentrated with Lenti-X Concentrator (Clontech, Fermont CA) 48 and 72 h post-transfection. The recombinant lentivirus particles were first infected into Panc02-H7 cells grown to 50% confluence; the medium was changed to the normal culture medium 12 h post infection. A limited dilution method was used to generate single cell clones. Each clone was amplified and the level of CDH17 mRNA expression in each cell clone was measured with qPCR. The resultant stable cell clones with significant CDH17 suppression were named as CDH17-shRNA-Panc02-H7 cells.

2.7. Using CRISPR technology to establish stable CDH17 knockout cells

To knock out CDH17 with CRISPR technology, we first transfected LentiCas9-EGFP plasmids to Panc02-H7 cells to establish stable Cas9-expressing cell clones with the method described above. The crRNAs specific for CDH17 and tracrRNAs were designed with online software, CRISPR DESIGN (http://crispr.mit.edu) and synthesized with IDT (Coralville, IA). 1 μl each of crRNA (100 μM), tracrRNA (100 μM), and 18 μl nuclease-free water were mixed and heated to 95 °C for 5 min then cooled down to room temperature to form guide RNA duplex (gRNA). The resultant gRNAs were transfected into stable Cas9-Panc02-H7 cells with RNAi-MAX Lipofectamine (Invitrogen, Carlsbad, CA). Single-cell clones were generated with limited dilution as described above. Genomic DNAs from individual cloned cells were extracted using an SV genomic DNA kit (Promega, Madison, WI). Using genomic DNA as a template, we amplified targeted CDH17 DNA fragments with specific primers. The DNA fragments were digested with T7 endonuclease 1 to evaluate cutting efficiency mediated by cas9 and gRNA. Sanger DNA sequencing identified the specific base-depleted site in the targeted DNA fragment. qPCR to measure mRNA expression was used to validate

CDH17 knockout. The final confirmed stable CDH17-knockout cells were named as CDH17-CRISPR-Panc02-H7 cells.

2.8. Establishing an orthotopic murine model of PC

PC cells grown to 90% confluence were harvested and suspended in 15% Matrigel in PBS; subsequently, these cells were injected into the head of the pancreas of wild-type C57BL/6 mice at a dose of 2.5×10^5 per mouse.

2.9. Proliferation and apoptosis detection

Cells grown to 90% confluence were harvested and seeded in a 96-well plate at a dose of 2×10^3/well and 8×10^3/well. At the indicated times, cell proliferation and apoptosis were measured with Proliferation Assay Kit (Promega, Madison, WI) and Apo-one Homogeneous Caspase-3/7 Assay kit (Promega, Madison, WI), according to the manufacturer's instructions.

2.10. Colony formation assay

Cells grown to 90% confluence were harvested and seeded in 6-well plate at a dose of 200 cells per well. Seven to 10 days later, cells were rinsed in PBS and stained with 0.05% crystal violet for photography and colony counting.

2.11. Wound healing assay

Cells grown to 90% confluence were harvested and seeded into 24-well plate with an insert at a density of 2×10^5 cells per well. The insert was removed carefully on the second day. The cell-free gaps were measured over time, with an optical microscope (Zeiss).

2.12. Total RNA extraction and qPCR

Total RNAs were extracted with Trizol reagent (Invitrogen, Carlsbad, CA). Reverse transcription of RNA to cDNA was conducted with High Capacity cDNA Reverse Transcription Kits (Applied Biosystems, Foster City, CA). qPCR was performed with QuantStudio 3 Detection System (ABI, Thermo Fisher) in a 20 μL reaction mixture containing SYBR Green I. Expression of different genes was normalized to housekeeping gene 18S rRNA, and further analyzed using the $2^{-\Delta\Delta CT}$ method.

2.13. Western blot analysis

Cell or tumor lysate was respectively prepared with lysis protein extraction reagent (Thermo Fisher Scientific, Inc) and M-PERTM mammalian protein extraction reagent (Thermo Fisher Scientific, Inc). After quantitating, an equal amount of proteins were loaded to perform western blotting as previously described [18,23].

2.14. Lifespan analysis

Mice were monitored for the development of ascites, impairment of gait and breathing, indicative of end-stage pancreatic tumors. Survival curves were constructed with the Kaplan-Meier method via GraphPad Prism software. Significance was determined by single-factor analysis of variance and validated using the log-rank test. p values of < 0.05 were considered significant.

2.15. Immunohistochemistry (IHC)

To make tumor tissue sections, PC tumor tissues, harvested from tumor-bearing mice, were fixed in formalin for at least 12 h, followed by dehydration with different grades of alcohol and chloroform: alcohol mixture, and embedded in paraffin. The resultant formalin-fixed paraffin embedded (FFPE) blocks were used to make 4-μm tissue sections. To conduct IHC, tissue sections were de-paraffinized with xylene, rehydrated with various grades of alcohol (100%, 95%, 80% and 70%), antigen unmasked with solution (Cat#: H-3300, Vector Laboratories), permeabilized with 0.2% Triton X-100, blocked with serum, then incubated with BLOXALL reagent (Cat#: SP-6000, Vector Laboratories) to quench endogenous peroxidase. Subsequently, the sections were incubated in succession with primary antibodies at optimized concentration, secondary antibody, and DAB substrate to develop color.

2.16. Statistics analysis

Paired data were analyzed using a 2-tailed paired student's t-test. A p value of < 0.05 was considered significant [24].

3. Results

3.1. Different levels of CDH17 expression in distinct PC cells and their derived orthotopic tumors

To investigate the role of CDH17 in PC tumor growth [15], we first examined CDH17 expression in different PC cell lines and their derived tumors. Using two mouse PC cell lines, including Panc02 and Panc02-H7 cells, we established their orthotopic murine model by injecting the cells into the head of the pancreas in wild-type C57BL/6 mice at a dose of 2.5×10^5 cells per mouse (Fig. 1A). At 17 days post inoculation, the average weight of tumors in each mouse induced by Panc02-H7 cells was 1.443 g, which was significantly greater than 0.298 g induced by Panc02 cells (Fig. 1B and C), suggesting tumors derived from Panc02-H7 cells grow much faster than those from Panc02 cells. We harvested Panc02 and Panc02-H7 cells, as well as their derived tumors, to extract total RNA and protein. qPCR showed that the expression of CDH17 mRNA is slightly higher in Panc02-H7 cells compared to that in Panc02 cells (Fig. 1D). However, CDH17 expression in orthotopic PC tumors induced by Panc02-H7 cells was 3-fold higher than the tumors derived from Panc02 cells (Fig. 1D). Western blot revealed that the level of CDH17 protein expression in the tumors derived from Panc02-H7 cells was much higher than the tumors derived from Panc02 cells (Fig. 1D). The different levels of CDH17 mRNA and protein (Fig. 1E) expressions were also detected in three human PC cell lines with the highest expression in Panc-1 cells. In addition, the results from the human database demonstrate a higher level of CDH17 expression in human PC tumors compared to that in normal human pancreases (Fig. 1 in Data in Brief). These data exhibit a positive relationship between CDH17 expression and tumor growth, suggesting the potential effect of CDH17 in advancing tumor progression.

3.2. siRNA, shRNA, and CRISPR-mediated knockdown or knockout of CDH17 in Panc02-H7 cells and establishment of the corresponding stable cell lines

To study the role of CDH17 in PC tumorigenesis, we first induced CDH17 knockdown in Panc02-H7 cells with RNA interference (siRNA). In doing so, three designed siRNAs for CDH17 were transfected into Panc02-H7 cells (Fig. 2A). As shown, all three siRNAs could inhibit CDH17 mRNA expression to a different extent compared to negative control (NC) siRNAs. A maximum suppressive effect was observed in siRNA-3 (Fig. 2B) where CDH17 mRNA expression was decreased to about 30% of that in NC siRNA-transfected cells. Therefore, we selected siRNA-3 for the following studies. Also, we demonstrated that siRNA-mediated CDH17 suppression is able to last at least 10 days (Fig. 2 in Data in Brief). Using the same strategies, we successfully conducted siRNA-mediated knockdown and recombinant plasmid-mediated ectopic expression in human Mia-Paca-2, human Panc-1 cells, and mouse Panc02-H7 cells (Fig. 3 in Data in Brief).

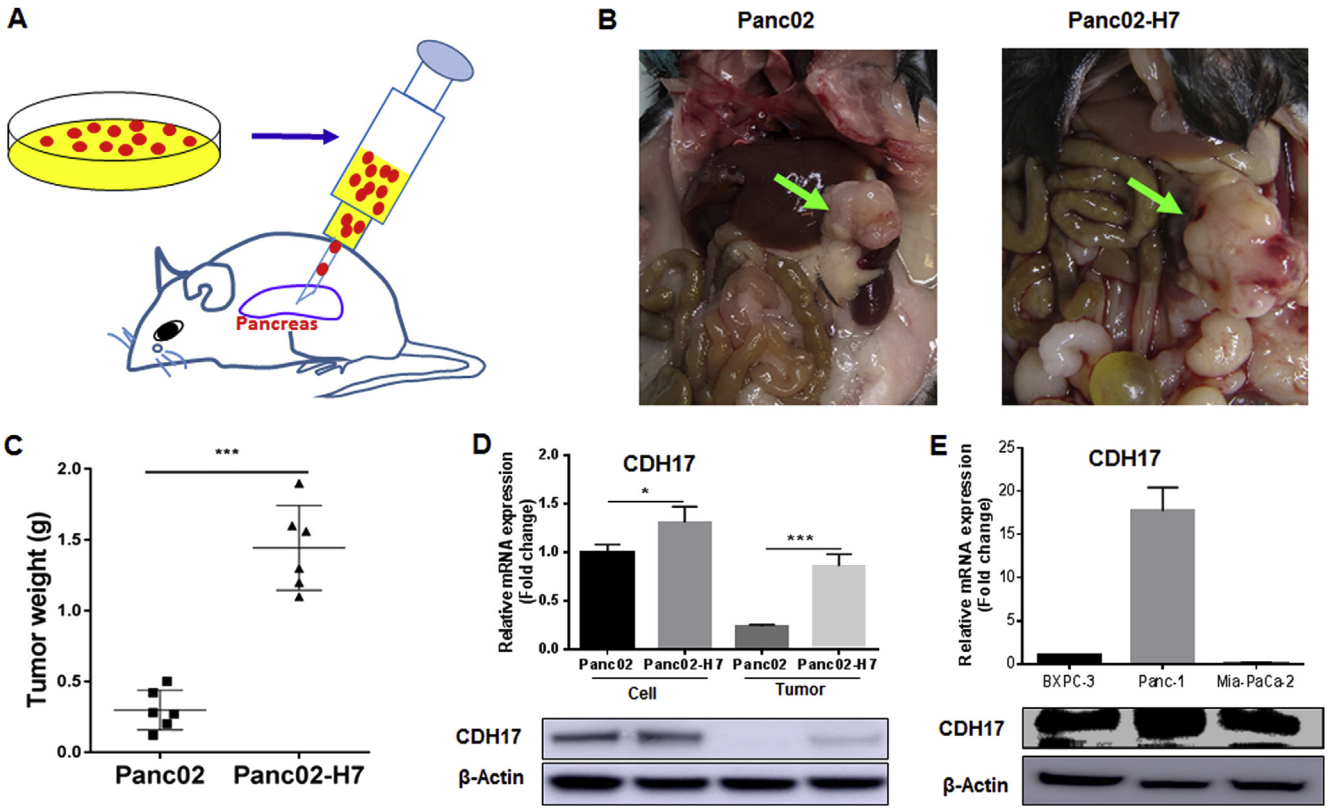

Fig. 1. CDH17 expression in mouse and human PC cells as well as the tumors. (A) Establishing an orthotopic murine model of PC in wild-type C57BL/6 mice. Panc02 or Panc02-H7 cells grown to 90% confluence were harvested and re-suspended in 15% Matrigel. These cells were injected into the head of the pancreas in wild-type C57BL/6 mice at a dose of 2.5×10^5 cells per mouse. (B) The representative images of orthotopic PC tumors in wild-type C57BL/6 mice induced with Panc02 and Panc02-H7 cells. 17 days post-injection of Panc02 and Panc02-H7 cell, all mice were euthanized for macroscopic examination of tumors. Observable orthotopic tumors were seen in all mice and are indicated by green arrows. (C) The accumulated tumor weights. (D) Levels of CDH17 mRNA and protein expression in mouse Panc02 and Panc02-H7 cells as well as their derived orthotopic PC tumors. Panc02 or Panc02-H7 cells grown to 90% confluence were harvested to extract total RNAs and prepare cell lysate. These cells were injected into the pancreas of wild type C57BL/6 mice to grow tumors. The tumors were harvested 17 days post cell inoculation and used to extract total RNAs and prepare tumor lysate. qPCR and western blot detected the higher expression of CDH17 in Panc02-H7 cells and their derived tumors relative to that in Panc02 cells and the derived tumors. (E) Levels of CDH17 mRNA and protein expression in human PC cells. Three human PC cell lines include BXPC-3, Panc-1, and Mia-Paca-2 were grown to 90% confluence, then harvested to extract total RNAs and prepare cell lysate. qPCR and western blot detected much higher mRNA and protein expression of CDH17 in Panc-1 cells compared to that in human BXPC-3 and Mia-Paca-2 cells.

Based on siRNA-3, we designed CDH17-shRNA and used it to establish stable CDH17-knockdown cells [25]. To this end, CDH17-shRNAs were inserted into plasmid pLL3.7 to construct recombinant CDH17-shRNA plasmids, which were subsequently co-transfected into HEK293 cells together with helper plasmid pMD2.G and psPAX2 to make recombinant CDH17-shRNA-lentivirus particles. The generated CDH17-shRNA recombinant lentivirus particles were transfected into Panc02-H7 cells followed by the screening of single transfected cell clones with limited dilution (Fig. 2C). Expression of CDH17 in each cell clone was detected with qPCR. The results revealed that CDH17 mRNA expression in the clones 4 and 5 was significantly decreased to 40% of that in the scrambled shRNA-transfected cells (Fig. 2D). Western blotting further validated this reduction in protein level (Fig. 2E), suggesting successful CDH17-knockdown in Panc02-H7 cells. This cell clone was named CDH17-shRNA- Panc02-H7.

Further, we used CRISPR technology to establish stable CDH17-knockout cells. As described in the materials and methods section, we designed CRISPR RNA probes, made gRNA for CDH17, and then transfected it into stable Cas9-Panc02-H7 cells to generate single-cell clones with the limited dilution (Fig. 2F). Each single-cell clone was expanded and CDH17 mRNA expression measured with qPCR. The results demonstrated that CDH17 mRNA expression was significantly reduced in cell clones 2, 5, 10, and 12, and was almost undetectable in clone 10 (Fig. 2G). Western blot validated this result, as no CDH17-positive band was detected in cell clone 10 (Fig. 2H). Sanger DNA sequencing further demonstrated that 65 bases were depleted from the CDH17 gene (Fig. 2I), suggesting successful CDH17-knockout in this clone. This cell clone 10 was named CDH17-CRISPR-Panc02-H7.

3.3. Knockdown or knockout of CDH17 causes growth and clonogenic survival suppression in mouse and human PC cells

Using the validated CDH17-siRNA, stable CDH17-knockdown, and CDH17-knockout cells, we first investigated the effect of CDH17 in Panc02-H7 cell growth. CDH17-siRNA-transfected Panc02-H7 cells (one day after transfection), stable CDH17-shRNA-Panc02-H7 cells grown to 80% confluence, and CDH17-CRISPR-Panc02-H7 cells grown to 80% confluence along with their respective control cells were seeded into 96-well plate, respectively. On days 1 and 2, MTT assay were used to examine Panc02-H7 cell proliferation following manufacturer's instruction (Fig. 3A). The results show that knockdown of CDH17 with siRNA leads to a significant reduction of cell viability to 60% on day 1 and 80% on day 2 compared to the control cells (Fig. 3B). This CDH17 defect-mediated growth suppression was further confirmed by stable CDH17-shRNA-Panc02-H7 cells and CDH17-CRISPR-Panc02-H7 cells, as the viability of both stable cells was reduced to 60% on day 1 and 45% on day 2 (Fig. 3C and D). siRNA-mediated CDH17 knockdown also caused suppression of cell proliferation and clonogenic formation in human Mia-Paca-2 and Panc-1 cells (Fig. 4 in Data in Brief). In contrast, ectopic expression of CDH17 advanced proliferation and clonogenic

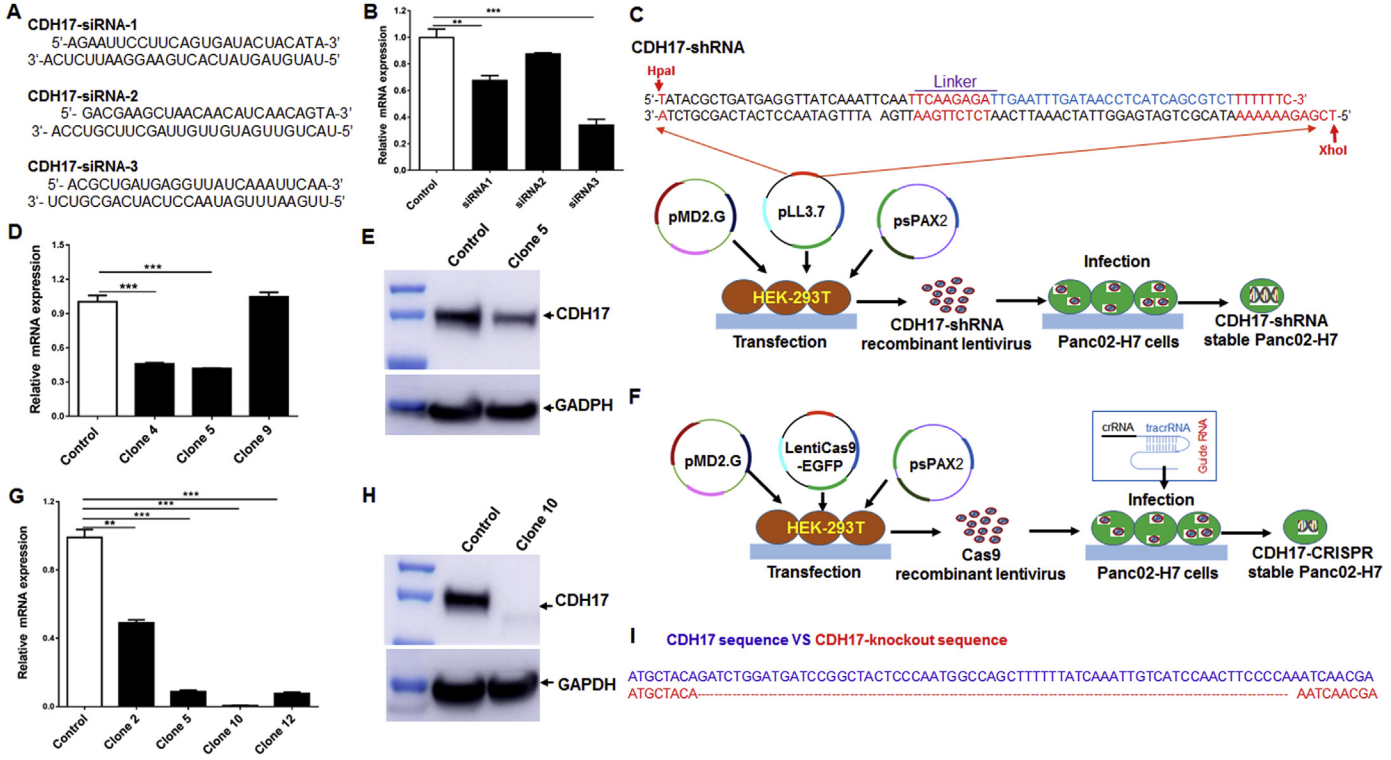

Fig. 2. Knockdown or knockout of CDH17 in PC cells with siRNA, shRNA, and CRISPR technology. 1×10^5 Panc02-H7 cells were seeded in each well of a 6-well plate and transfected with the indicated siRNAs with RNAi-MAX Lipofectamine reagent on the second day. On the third day, the cells were harvested to extract total RNA to detect CDH17 mRNA expression with qPCRs. NC siRNAs were used for control. (A) The sequences of three siRNAs for CDH17 from IDT. (B) The effect of three siRNAs on CDH17 mRNA expression in Panc02-H7 cells. Each siRNA was transfected into Panc02-H7 cells with Lipofectamine RNAiMAX (Invitrogen). 36 h post-transfection, the total RNAs were extracted from the transfected cells. qPCR was used to detect the expression of CDH17 mRNA; the results showed that siRNA-3 led to the reduction of CDH17 mRNA expression to 35% of that in the cells transfected with NC siRNAs. (C) Establishing CDH17-knockdown stable cells with shRNAs. CDH17-shRNA was designed upon CDH17-siRNA-3 sequences. Two complementary chains of CDH17 oligonucleotides were synthesized and annealed to form double chain DNA fragments, which were cloned into vector pLL3.7 between *Hpa*I and *Xho*I sites. The recombinant plasmids, or scrambled shRNA plasmid together with helper plasmids pMD2.G and psPAX2, were transfected into HEK293 cells in which the CDH17-shRNA-recombinant lentivirus or scrambled shRNA lentivirus were packaged to form virus particles. The virus particles were then infected into Panc02-H7 cells. The transfected cells were diluted on the second day and seeded into each well to get single cell clones. (D) shRNA-mediated CDH17 knockdown in stable Panc02-H7 cell clones. qPCR showed that the CDH17 mRNA level in clones 4 and 5 was reduced to about 40% of that in scrambled shRNA control cells. Clone 5-amplified cells were named as CDH17-shRNA-Panc02-H7 cells. (E) CDH17 protein expression in stable CDH17-shRNA-Panc02-H7 cells. Western blot detected the reduced CDH17 protein in stable CDH17-shRNA-Panc02-H7 cells relative to control cells. (F) Establishing stable CDH17 knockout in Panc02-H7 cells with CRISPR technology. Following manufacturer's instructions, we first transfected the Cas9 recombinant plasmids to Panc02-H7 cells to establish single Cas9-expressing stable cell lines as described in C. The designed gRNAs for CDH17 were transfected into stable Cas9-Panc02-H7 cells with RNAi-MAX Lipofectamine (Invitrogen). The transfected cells were diluted on the second day and seeded into each well to get single cell clones. (G) CRISPR-mediated knockout of CDH17. qPCR detected the suppressed expression of CDH17 in cell clones 2, 5, 10, and 12 with almost no detectable CDH17 in clone 10. Clone 10-amplified cells were named as CDH17-CRISPR-Panc02-H7 cells. (H) CDH17 protein expression in CDH17-CRISPR-Panc02-H7 cells. Western blot showed no observable CDH17 protein was detected in stable CDH17-CRISPR-Panc02-H7 cells relative to vehicle control cells. (I) Sanger DNA sequencing was performed to validate CDH-17 knockout.

formation of human Mia-Paca-2 cells with low CDH17 expression (Fig. 4A and C in Data in Brief), but this effect was not observed in human Panc-1 cells with high CDH17 expression (Fig. 4B and D in Data in Brief).

To further test if CDH17 disruption reduces clonogenic survival of Panc02-H7 cells, *in vitro* colony formation assays were performed as described in the materials and methods section [26]. The results demonstrated that siRNA-mediated CDH17 knockdown significantly reduced Panc02-H7 cell colony numbers from 160 to 80 relative to control cells (Fig. 3E and F). This reduction was also observed in stable CDH17-shRNA-Panc02-H7 cells (Fig. 3G and H) and CDH17-CRISPR-Panc02-H7 cells (Fig. 3I and J), as only 90 and 30 colonies were detected in these two stable cells. These results suggest that CDH17 disruption significantly inhibited Panc02-H7 cell growth and anchorage-free colony formation.

3.4. Knockdown or knockout of CDH17 can suppress Panc02-H7 cell motility

Next, a wound healing assay was conducted to investigate if the CDH17 gene plays a critical role in modulating PC cell migration. Cells including CDH17-siRNA-transfected Panc02-H7 cells (24 h after transfection), stable CDH17-shRNA-Panc02-H7 cells grown to 80% confluence, and CDH17-CRISPR-Panc02-H7 cells grown to 80% confluence as well as their respective control cells were seeded in an insert-containing 24-well plate at a dose of 2×10^5 cells per well. On the second day, the insert was removed. The cell-free gaps were measured at the indicated time after the insert was removed. The representative (Fig. 4A) and accumulated (Fig. 4B) results show that siRNA-mediated CDH17 knockdown significantly suppressed Panc02-H7 cell migration. Cell-free gaps measured in siRNA-CDH17 knockdown cells, 12, 24, and 36 h after removing the insert, were 415 μm, 370 μm, and 155 μm, respectively. These cell-free gaps were markedly wider compared to 346 μm, 250 μm, and 0 μm in control cells transfected with NC siRNAs.

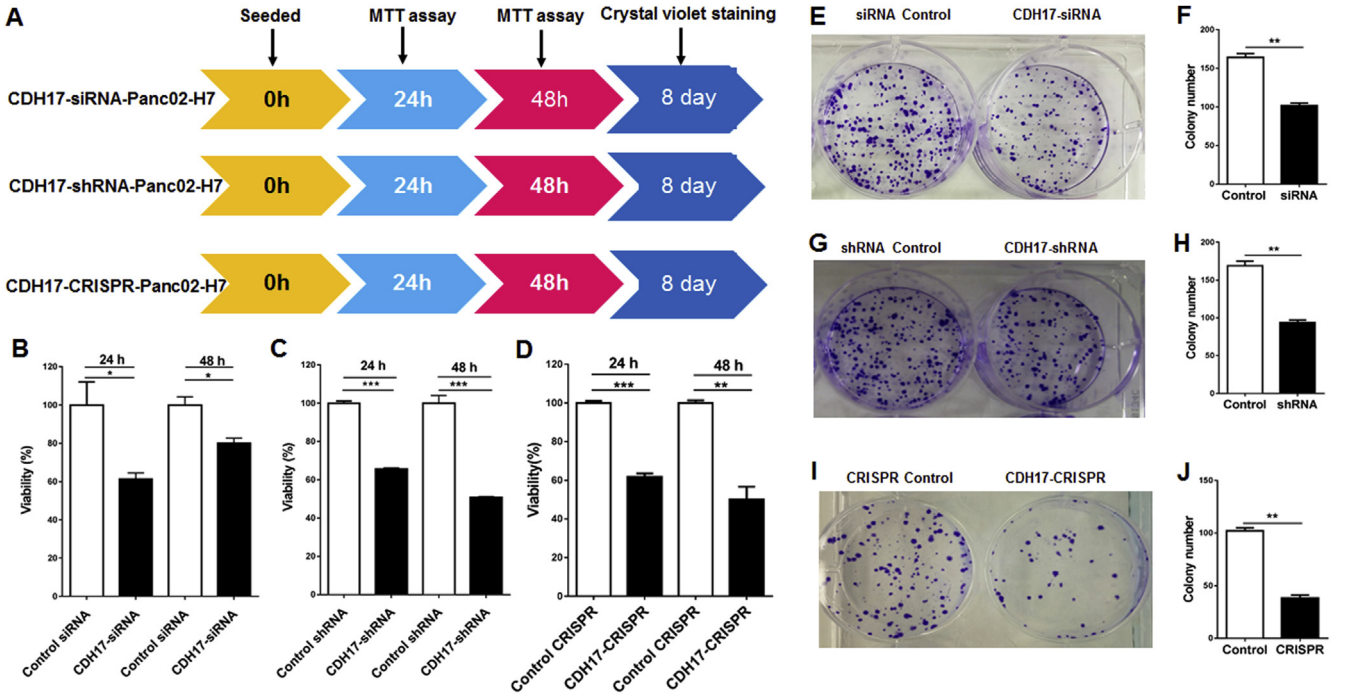

Fig. 3. Knockdown and knockout of CDH17 suppresses Panc02-H7 cell proliferation and inhibits cell colony formation. (A) Outline of cell proliferation and colony formation assay. The Panc02-H7 cells were transfected with CDH17-siRNA-3. One day later, the transfected cells were seeded into 96-well plate at a dose of 2×10^3 cells/well or 6-well plate at a dose of 2×10^2 cells/well for viability and colony formation assays. Similar procedures for cell proliferation and colony formation at the same dose and timeline were performed in stable CDH17-shRNA-Panc02-H7 or stable CDH17-CRISPR-Panc02-H7 cells grown to about 90% confluence. MTT assay was used to measure cell viability for CDH17-siRNA-transfected Panc02-H7 cells (B), stable CDH17-shRNA-Panc02-H7 (C), and stable CDH17-CRISPR-Panc02-H7 (D) cells at 24 or 48 h post cell seeding. Crystal violet staining was used to define the colony formation by counting the numbers of cell colonies eight days post cell seeding. Representative images of colony formation and average numbers of cell colony were shown for CDH17-siRNA-transfected Panc02-H7 cells (E) and (F), stable CDH17-shRNA-Panc02-H7 cells (G) and (H), or CDH17-CRISPR-Panc02-H7 cells (I) and (J). n = 3, error bars represent mean ± SD.

The stronger suppression of cell migration was also detected in stable CDH17-shRNA-Panc02-H7 cells (Fig. 4C and D) and CDH17-CRISPR-Panc02-H7 cells (Fig. 4E and F), as the cell-free gaps seen in both stable cells were wider than that in each control cell. Similarly, siRNA-mediated CDH17 knockdown resulted in the suppression of cell migration in human PC Mia-Paca-2 (Fig. 5A in Data in Brief) and Panc-1 (Fig. 5B in Data in Brief) cells. In contrast, ectopic expression of CDH17 prompted the migration of human Mia-Paca-2 cells with low CDH17 expression (Fig. 5A in Data in Brief), but this effect was not observed in human Panc-1 cells with high CDH17 expression (Fig. 5B in Data in Brief). These results suggest that disruption of CDH17 is able to significantly inhibit PC cell migration.

3.5. CDH17-knockdown or knockout in Panc02-H7 cells slows orthotopic PC tumor growth in recipient wild-type mice and extends their lifetime

Because defects in CDH17 comprehensively influence Panc02-H7 cell function and behavior *in vitro,* we investigated its effect on orthotopic tumor growth *in vivo*. Three cell types, including CDH17-siRNA-transfected Panc02-H7 cells (24 h post transfection), stable CDH17-shRNA-Panc02-H7 cells grown to 80% confluence, and CDH17-CRISPR-Panc02-H7 cells grown to 80% confluence as well as their respective control cells, were harvested and injected into the head of the pancreas of wild-type C57BL/6 mice at a dose of 2.5×10^5 cells per mouse. All mice were euthanized 17 days later for harvesting the tumors and other organs. The average weight of the tumors induced by CDH17-siRNA-transfected Panc02-H7 cells was roughly 1.12 g, which was lighter than the tumors induced by NC siRNAs-transfected Panc02-H7 cells with an average weight of about 1.38 g (Fig. 5A and B). The results show that knockdown of CDH17 with siRNAs slows orthotopic tumor growth compared to that in wild-type mice receiving NC siRNA-transfected Panc02-H7 cells. More noticeable suppression of tumor growth was seen in tumor-bearing mice induced by stable CDH17-knockdown Panc02-H7 cells and stable CDH17-knockout Panc02-H7 cells. As shown, average tumor weight of 0.5 g vs 0.94 g (Fig. 5D and E) and 0.24 g vs 0.41 g (Fig. 5G and H), were detected in the mice receiving stable CDH17-shRNA-Panc02-H7 cells, stable CDH17-CRISPR-Panc02-H7 cells, and their controls, respectively.

Given the significant effect of CDH17 knockdown and knockout on tumor growth, CDH17 disruption is likely to impact the lifespan of tumor-bearing mice [18]. To test this hypothesis, we prepared orthotopic tumor-bearing mice, as described above, with CDH17-siRNA-transfected Panc02-H7 cells, stable CDH17-shRNA-Panc02-H7 cells, and CDH17-CRISPR-Panc02-H7 cells, respectively. Mice were monitored every day for the development of ascites and impairment of gait and breathing, indicative of end-stage pancreatic tumors. Based on these criteria, viable mice were counted over time. Survival curves were constructed with the Kaplan-Meier method using GraphPad Prism software. The results showed that the average survival time of tumor-bearing mice derived from CDH17-siRNA-transfected cells wasroughly 28.5 days, significantly longer than 18.5 days in mice with tumors induced by NC siRNA-transfected Panc02-H7 cells (Fig. 5C). Similarly, the average survival time of tumor-bearing mice induced by stable CDH17-shRNA-Panc02-H7 cells and CDH17-CRISPR-Panc02-H7 cells was 26 days (Fig. 5F) and 33 days (Fig. 5I), respectively. Both were longer than 19 days and 22 days in mice with tumors induced with control cells. These data demonstrate that CDH17 knockdown or knockout in Panc02-H7 cell not only slows orthotopic tumor growth *in vivo* but also significantly extends the lifespan of tumor-bearing mice derived from these cells.

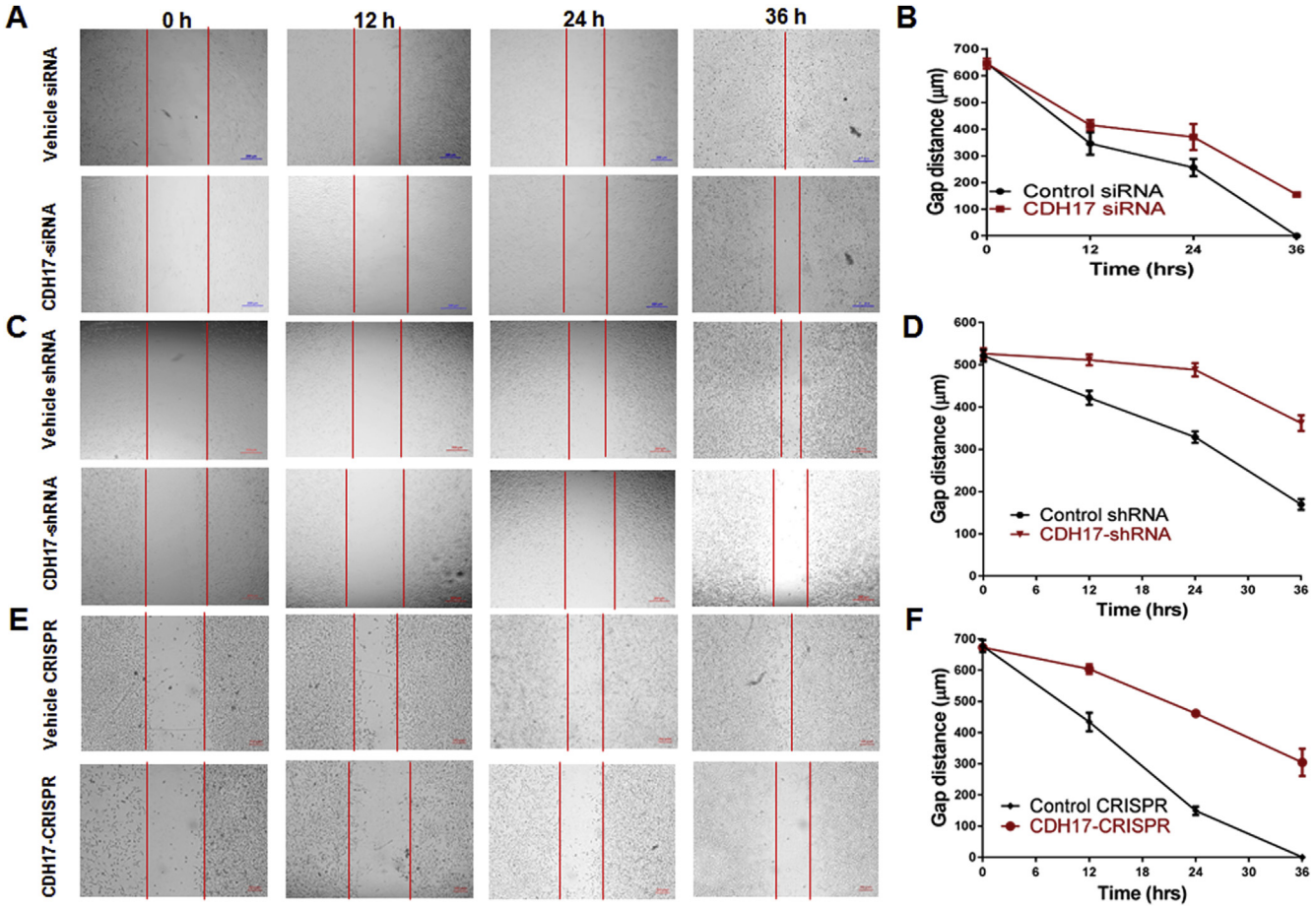

Fig. 4. CDH17 knockdown and knockout suppress cell motility. CDH17-siRNA-transfected Panc02-H7 cells, stable CDH17-shRNA-Panc02-H7 cells, or stable CDH17-CRISPR-Panc02-H7 cells, as well as their controls, were prepared as described in Fig. 3, then seeded into 24-well plate at a dose of 2×10^5 cells/well, respectively. The insert in each well was removed on the second day. The cell-free gap was measured at the indicated times. Representative images of cell-free gaps and average widths of gaps were shown for siRNA-knockdown Panc02-H7 cells (A) and (B), stable CDH17-shRNA-Panc02-H7 cells (C) and (D), or CDH17-CRISPR-Panc02-H7 cells (E) and (F). n = 3, error bars represent mean ± SD.

3.6. CDH17 disruption suppresses Akt and Bcl-2 pathways and causes apoptotic PC cell death

Having validated CDH17's oncogenic effect in PC, we subsequently tried to elucidate the underlying molecular mechanism. Using CDH17 knockdown and knockout cells, we first investigated the correlation of CDH17 disruption and PC cell apoptosis by measuring the activities of caspase-3 and -7 with Apo-one Homogeneous Caspase-3/7 Assay kit. The results showed that the caspase-3 and -7 activities were significantly increased in stable CDH17-knockout cells, evidenced by the stronger fluorescence measured in CDH17-CRISPR-Panc02-H7 cells compared to that in control cells (Fig. 6A). Similarly, an increase of caspase-3 and -7 activity was also detected in stable CDH17-shRNA-Panc02-H7 cells (data not shown). Subsequently, using western blot, we detected the level of a panel of well-characterized signaling molecules, relevant to cell growth, in CDH17-defect cells. We verified that the Bcl-2 and phosphorylated Akt were markedly reduced in stable CDH17-shRNA-Panc02-H7 cells and CDH17-CRISPR-Panc02-H7 cells compared to that in either control cells (Fig. 6B). Additionally, CDH17 disruption caused the increased expression of Bax, Bad, Cleaved PARP, Cleaved caspase 3, and Cytochrome C in the CDH17-CRISPR-Panc02-H7 cells relative to that in control cells (Fig. 6C). IHC staining revealed decreased Ki67 and increased cleaved caspase 3 in tumors induced with CDH17-CRISPR-Panc02-H7 cells (Fig. 6C) compared to tumors derived with their control cells. In addition, we examined the expression of other cadherin family members in tumors induced by Panc02-H7 cells and defined their correlation with CDH17 knockout. IHC detected strong positive staining for E-cadherin and N-cadherin in tumors induced with Panc02-H7 cells, both of them were markedly reduced in the tumors induced with CDH17-knockout cells. In contrast, no positive signal was detected for CDH16 in the tumors derived with either control or CDH17-knockout Panc02-H7 cells (Fig. 6 in Data in Brief). These data are consistent with the report from the GEPIA online database (Fig. 1 in Data in Brief). These results suggest that impairing CDH17 suppresses PC growth by inducing a pro-apoptotic effect in PC, and this effect is associated with modulation of cell survival and apoptosis-signaling pathways (Fig. 6E). Together, these comprehensive studies underline that CDH17 functions as a critical molecule in PC progression and could be targeted to develop an anti-PC therapy.

4. Discussion

To our knowledge, this is the first report describing CDH17 functions as a critical oncogenic gene modulating PC growth [27]. Using a loss-of-function strategy, we have demonstrated that CDH17 is necessary to maintain PC cell tumorigenic activity *in vitro* and to advance tumor growth *in vivo*. These findings significantly advance our understanding of CDH17 action in PC and provide a potential target to develop an anti-PC therapeutic strategy.

Using a loss-of-function strategy, we investigated how CDH17 disruption impacts PC proliferation, colony formation, and migration *in vitro,* and tumor growth *in vivo*. We have now demonstrated that siRNA-

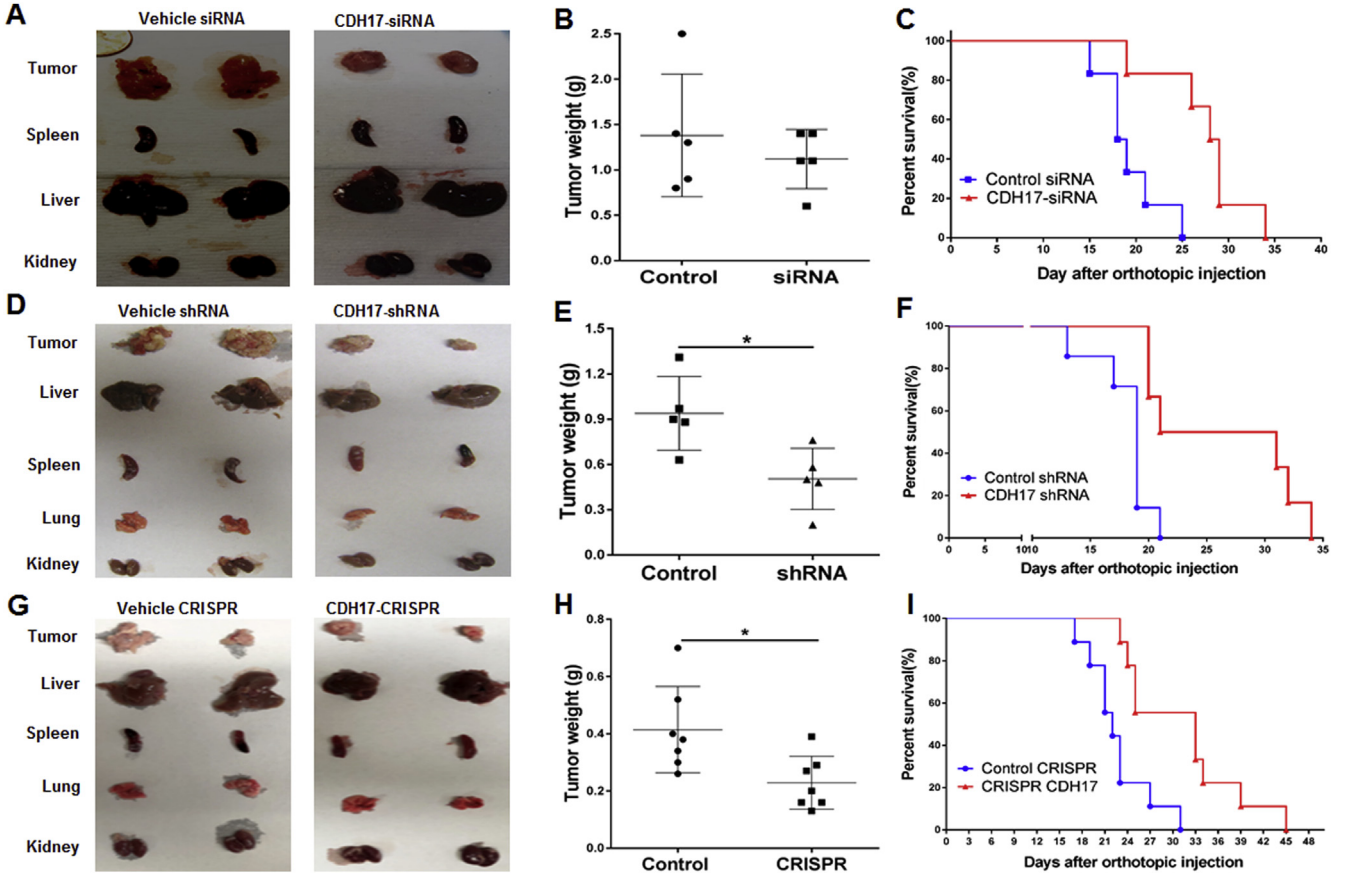

Fig. 5. Knockdown and knockout of CDH17 in Panc02-H7 cells induce suppression of orthotopic tumor growth. CDH17-siRNA-transfected Panc02-H7 cells, stable CDH17-shRNA-Panc02-H7 cells, or stable CDH17-CRISPR-Panc02-H7 cells, as well as their relative controls, were prepared and harvested as described in Fig. 3; each type of the harvested cells was injected into the head of a pancreas of C57BL/6 mice at a dose of 2.5×10^5 cells per mouse. Half of these mice were used to detect tumor growth; the other half were used for lifespan monitoring. To detect tumor growth, 17 days later, each mouse was euthanized, tumors and various organs were harvested, and the tumors were weighed. To monitor the lifespan, the viable mice were counted over time, and the survival curves were made using the Kaplan-Meirer method. The representative images of tumors and organs (spleen, and liver, and kidney), accumulated tumor weights, and lifespan are shown in mice receiving CDH17-siRNA-transfected Panc02-H7 cells (A–C), stable CDH17-shRNA-Panc02-H7 cells (D–F), or CDH17-CRISPR-Panc02-H7 cells (G–I). n = 5 (tumor weight) or 7 (lifespan), error bars represent mean ± SD.

mediated CDH17 knockdown significantly suppresses PC cell growth including its proliferation and clonogenic survival (Figs. 2A, 3B and 3E). This effect is more obviously observed in the stable CDH17-knockdown cells (Fig. 2D–F, 3C, 3G) and CDH17-knockout cells (Fig. 2G–I, 3D, 3I). We also demonstrated that CDH17-knockdown and knockout effectively suppress PC cell migration, as a wound healing assay showed that siRNA-mediated CDH17-knockdown markedly slowed PC cell motility (Fig. 4A). Most importantly, knockdown or knockout of CDH17 in PC cells significantly suppressed orthotopic tumor growth in the recipient wild-type mice (Fig. 5A–I). These results suggest that CDH17 exerts a tumor-promoting and carcinogenic effect. This finding in PC is consistent with recent and previous outcomes observed in colon, melanoma, and breast cancer cell lines [28]. In 2013, one group reported that blocking or impairing CDH17 signaling pathways was able to suppress gastric cancer growth [12]. In 2018, another group generated highly selective antibodies against RGD motifs in CDH17. This antibody is able to block CDH17 activation and provoke a significant reduction in cell adhesion and proliferation of several types of metastatic cancer cells [29,30]. One group detected the upregulation of CDH17 in human liver cancers and demonstrated that CDH17 was able to transform premalignant liver progenitor cells to produce liver carcinomas in mice. RNA interference-mediated knockdown of CDH17 inhibited proliferation of both primary and highly metastatic HCC cell lines *in vitro* and *in vivo* [19]. Taken together, our results identify CDH17 as a novel oncogene in PC.

Signaling through CDH17 contributes to multiple PC-associated processes such as cell proliferation, colony formation, and cell invasion. The underlying mechanisms are completely unknown. Considering its oncogenic characteristics in PC, we investigated CDH17-mediated signal transduction on cell growth and death by investigating CDH17-responsive survival and apoptosis targets. We demonstrated that CDH17 disruption mediated by siRNA, shRNA, or CRISPR caused a marked reduction in the expression of Bcl-2, pAkt, and survivin in PC cells (Fig. 6B), these proteins are well-documented molecules and represent two main survival pathways, which contribute to cancer formation and progression [31]. Using stable CDH17 knockdown or knockout cells, we have detected CDH17 disruption resulted in a significant increase in the level of apoptotic proteins including cytochrome C, cleaved caspase 3, and cleaved PARP (Fig. 6C). Similarly, the increase of cleaved caspase 3 and reduction of Ki67 was also detected in tumors induced with CDH17-knockout cells (Fig. 6D). These data reveal that CDH17 functions as an oncogenic molecule in PC and exerts its function by regulating Akt, Bcl-2, and caspase-3 signaling pathways, which are critical for cell survival and apoptosis [32]. This finding is different from the mechanisms reported in gastric cancer and liver cancer. One study reported that CDH17 knockdown decreased β-catenin and GSK-3β phosphorylation, accompanied by a concomitant increase of Rb and reduction of Cyclin D1 in gastric cancer [12]. Another group reported that RNA interference-mediated knockdown of CDH17 inhibited proliferation of both primary and highly metastatic

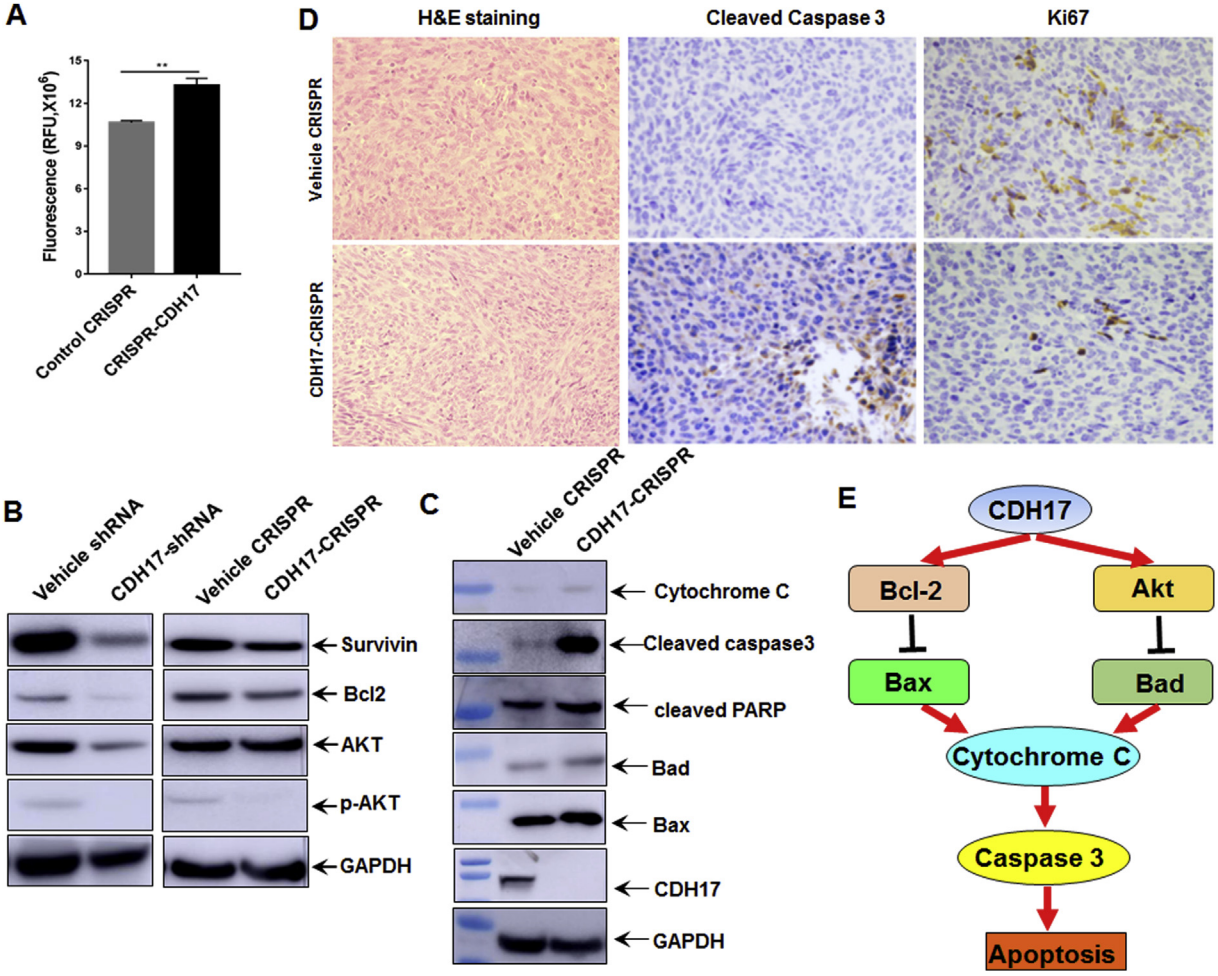

Fig. 6. CDH17 knockdown or knockout induces apoptotic Panc02-H7 cell death by suppressing Akt and Bcl-2 apoptotic pathways. (A) CDH17 knockout induces cell apoptosis. Stable CDH17-CRISPR-Panc02-H7 cells and the control cells were seeded into 96-well plate at a dose of 2×10^3/well. 12 h later, the activities of caspase-3 and -7 were measured with Apo-one Homogeneous Caspase-3/7 Assay kit. (B) Protein expression of canonical molecules important for cell survival. Stable CDH17-shRNA-Panc02-H7 cells and CDH17-CRISPR-Panc02-H7 cells, as well as their control cells grown to 90% confluence, were harvested and extracted protein. Western blot was used to detect the protein levels of Akt, p-Akt, Bcl-2, and Survivin in the indicated cells. (C) Protein expression of well-recognized molecules important for cell apoptosis. As performed in B above, the proteins extracted from stable CDH17-CRISPR-Panc02-H7 cells and vehicle control cells were used to conduct western blot for detecting protein expressional level of Bax, Bad, cleaved PARP, cleaved caspase 3, and cytochrome C. (D) Protein expression levels of cleaved caspase 3 and Ki67 in orthotopic PC tumors. Stable CDH17-CRISPR-Panc02-H7 cells and the control cells grown to 90% were used to induce orthotopic PC tumors in wild-type mice as described in the methods. 17 days post-inoculation, the tumors were harvested and then fixed with formalin to prepare slides. H&E staining showed tumor structure; IHC was performed to detect the expression of cleaved caspase 3 and Ki67. (E) A schematic diagram showing a signaling pathway of CDH17-mediated effect on PC cell growth. CDH17 suppresses Bax and Bad by stimulating Bcl-2 and Akt, and subsequently causes the suppression of cytochrome C and its downstream caspase 3, resisting PC cell apoptosis. In contrast, CDH17 impairment causes cell apoptosis.

HCC cell lines *in vitro* and *in vivo* involving inactivation of Wnt signaling [19]. Using nude mice, one study reported that miRNA-mediated CDH17 knockdown is responsible for the retention of NF-κB and a concomitant reduction of downstream proteins, suggesting the NF-κB signaling pathway may involve a CDH17-mediated effect on gastric cancer [17]. These data show that CDH17 exerts a tumorigenic effect on different types of cancer through inconsistent signaling pathways.

Our study also contributes to the identification of CDH17 as a potential therapeutic target in PC control. Our *in vitro* and *in vivo* experiments have demonstrated that CDH17 has an oncogenic role in PC, and CDH17 knockdown or knockout significantly suppresses orthotopic tumor growth in wild-type mice (Fig. 5). These results imply the potential of CDH17 as a therapeutic target. Recently, Dr. Casal's group used CDH17-RGD motif peptides to generate highly selective monoclonal antibodies (mAbs); treatment of colorectal- or melanoma-tumor-bearing mice with this antibody generated a promising therapeutic effect against advanced metastatic cancer by blocking the interaction of RGD and alpha 2 beta 1 integrin [30]. Another group reported that intra-tumor injection of CHD17 shRNAs resulted in significant anti-tumor therapeutic effects on transplanted tumor models [12]. In our study, we have identified effective siRNAs and shRNAs against CDH17; this will enable us to conduct anti-PC RNAi therapeutic studies. In addition, we have now developed a peptide-based nanoparticle with PC tumor-homing and penetrating characteristics. This nanoparticle has the capacity to load siRNA and to deliver it specifically to tumors. The first RNAi therapy for the polyneuropathy of hereditary transthyretin-mediated (hATTR) has been approved by the US FDA [33]. Further, it is reasonable for us to advance CDH17 siRNA therapy in PC treatment for rapid translation into clinical application.

CDH17 expression is positively correlated with tumor growth but is usually low in most types of cancer. Only colorectal cancers and several cases of stomach cancers display strong cytoplasmic and membranous positivity. With immunohistochemistry, Masaaki Takamura et al. detected strong expression of CDH17 in well-differentiated pancreas carcinoma, but not in differentiated areas and poorly differentiated carcinoma [34]. Using qPCR and immunofluorescence cytochemistry

assay, Wong et al. found that CDH17 was predominantly expressed in the cytoplasm of human HCC cells and HCC tumors, but not normal liver [35]. Their studies demonstrate that CDH17 expression is positively related with poor overall survival and disease-free survival times of human HCC [36]. Consistent with this conclusion, we have demonstrated the correlation of CDH17 expression with PC cell differentiation. Panc02-H7 cells are derived from Panc02 cells and are more invasive after *in vivo* passaging in wild-type mice for roughly ten times [37]. Real-time PCR and western blot detected a relatively high level of CDH17 RNA and protein expression in Panc02-H7 cells compared to Panc02 cells (Fig. 1D); this increased expression was also reflected in their derived tumors (Fig. 1D). Interestingly, Panc02-H7 cells had a faster tumor growth rate in wild-type mice relative to Panc02 cells (Fig. 1C). These findings suggest a positive correlation between CDH17 and PC tumor growth as well as poor prognosis. Our further studies demonstrated that CDH17 disruption caused growth suppression in both Panc02-H7 cells and their derived tumors. This solid evidence exhibits the critical role of CDH17 in well-differentiated PCs. However, we do not know if CDH17 exerts a similar effect in Panc02 cells with lower expression of CDH17 and human PC tumors. Therefore, further effort is required to expand our study to more distinct PC cells and their derived tumors. The results will inform us if a CDH17-mediated effect on PCs is cell-type-dependent and associated with the level of CDH17 expression.

In summary, our studies demonstrate, for the first time, the oncogenic activity of CDH17 necessary to maintain PC tumorigenesis. Disrupting CDH17 significantly suppresses PC development by regulating survival and apoptosis pathways. These findings significantly advance our understanding of CDH17 action in PC and offer a potential target for developing an anti-PC therapeutic strategy.

Financial support

This project was supported by a startup fund from the University of Missouri (Guangfu Li, PI) and in part by the Priority Academic Program Development of Jiangsu Higher Education Institutions, Nanjing Medical University, China.

Conflicts of interest

There is none to declare.

Appendix A. Supplementary data

Supplementary data to this article can be found online at https://doi.org/10.1016/j.canlet.2019.04.022.

References

[1] D. Qian, Z. Lu, Q. Xu, P. Wu, L. Tian, L. Zhao, B. Cai, J. Yin, Y. Wu, K.F. Staveley-O'Carroll, K. Jiang, Y. Miao, G. Li, Galectin-1-driven upregulation of SDF-1 in pancreatic stellate cells promotes pancreatic cancer metastasis, Cancer Lett. 397 (2017) 43–51.
[2] S.S. Vege, S.J. Pandol, Advances in pancreatic cancer, IPMN and pancreatitis, Gastroenterology 155 (3) (2018 Sep) 581–583.
[3] L. Rahib, B.D. Smith, R. Aizenberg, A.B. Rosenzweig, J.M. Fleshman, L.M. Matrisian, Projecting cancer incidence and deaths to 2030: the unexpected burden of thyroid, liver, and pancreas cancers in the United States, Cancer Res. 74 (2014) 2913–2921.
[4] R. Siegel, C. DeSantis, K. Virgo, K. Stein, A. Mariotto, T. Smith, D. Cooper, T. Gansler, C. Lerro, S. Fedewa, C. Lin, C. Leach, R.S. Cannady, H. Cho, S. Scoppa, M. Hachey, R. Kirch, A. Jemal, E. Ward, Cancer treatment and survivorship statistics, CA A Cancer J. Clin. 62 (2012) 220–241 2012.
[5] J. Ferlay, D.M. Parkin, E. Steliarova-Foucher, Estimates of cancer incidence and mortality in Europe in 2008, Eur. J. Cancer 46 (2010) 765–781.
[6] D. Ansari, C. Del Pino Bellido, M. Bauden, R. Andersson, Centrosomal abnormalities in pancreatic cancer: molecular mechanisms and clinical implications, Anticancer Res. 38 (2018) 1241–1245.
[7] C. Kratschmer, M. Levy, Targeted delivery of auristatin-modified toxins to pancreatic cancer using aptamers, Mol. Ther. Nucleic Acids 10 (2018) 227–236.
[8] C.L. Wolfgang, J.M. Herman, D.A. Laheru, A.P. Klein, M.A. Erdek, E.K. Fishman, R.H. Hruban, Recent progress in pancreatic cancer, CA A Cancer J. Clin. 63 (2013) 318–348.
[9] X. Qi, G. Li, D. Liu, A. Motamarry, X. Huang, A.M. Wolfe, K.L. Helke, D. Haemmerich, K.F. Staveley-O'Carroll, E.T. Kimchi, Development of a radiofrequency ablation platform in a clinically relevant murine model of hepatocellular cancer, Cancer Biol. Ther. 16 (2015) 1812–1819.
[10] D. Berndorff, R. Gessner, B. Kreft, N. Schnoy, A.M. Lajouspetter, N. Loch, W. Reutter, M. Hortsch, R. Tauber, Liver-intestine cadherin - molecular-cloning and characterization of a novel Ca2+-dependent cell-adhesion molecule expressed in liver and intestine, J. Cell Biol. 125 (1994) 1353–1369.
[11] A. Mokrowiecka, S. Zonnur, L. Veits, J. Musial, R. Kordek, M. Lochowski, J. Kozak, E. Malecka-Panas, M. Vieth, A. Hartmann, Liver-intestine-cadherin is a sensitive marker of intestinal differentiation during Barrett's carcinogenesis, Dig. Dis. Sci. 58 (2013) 699–705.
[12] H.B. Qiu, L.Y. Zhang, C. Ren, Z.L. Zeng, W.J. Wu, H.Y. Luo, Z.W. Zhou, R.H. Xu, Targeting CDH17 suppresses tumor progression in gastric cancer by downregulating Wnt/beta-catenin signaling, PLoS One 8 (2013) e56959.
[13] D.B. Ivanov, M.P. Philippova, V.A. Tkachuk, Structure and functions of classical cadherins, Biochemistry (Mosc.) 66 (2001) 1174–1186.
[14] S. Hirohashi, Y. Kanai, Cell adhesion system and human cancer morphogenesis, Cancer Sci. 94 (2003) 575–581.
[15] C. Grotzinger, J. Kneifel, D. Patschan, N. Schnoy, I. Anagnostopoulos, S. Faiss, R. Tauber, B. Wiedenmann, R. Gessner, LI-cadherin: a marker of gastric metaplasia and neoplasia, Gut 49 (2001) 73–81.
[16] B. Choi, H.J. Lee, J. Min, H.N. Choe, Y.S. Choi, Y.G. Son, H.S. Ahn, Y.S. Suh, J.R. Goldenring, H.K. Yang, Plasma expression of the intestinal metaplasia markers CDH17 and TFF3 in patients with gastric cancer, Cancer Biomark. 19 (2017) 231–239.
[17] J. Wang, W.M. Kang, J.C. Yu, Y.Q. Liu, Q.B. Meng, Z.J. Cao, Cadherin-17 induces tumorigenesis and lymphatic metastasis in gastric cancer through activation of NF kappa B signaling pathway, Cancer Biol. Ther. 14 (2013) 262–270.
[18] G. Li, D. Liu, T.K. Cooper, E.T. Kimchi, X. Qi, D.M. Avella, N. Li, Q.X. Yang, M. Kester, C.B. Rountree, J.T. Kaifi, D.J. Cole, D.C. Rockey, T.D. Schell, K.F. Staveley-O'Carroll, Successful chemoimmunotherapy against hepatocellular cancer in a novel murine model, J. Hepatol. 66 (2017) 75–85.
[19] L.X. Liu, N.P. Lee, V.W. Chan, W. Xue, L. Zender, C. Zhang, M. Mao, H. Dai, X.L. Wang, M.Z. Xu, T.K. Lee, I.O. Ng, Y. Chen, H.F. Kung, S.W. Lowe, R.T. Poon, J.H. Wang, J.M. Luk, Targeting cadherin-17 inactivates Wnt signaling and inhibits tumor growth in liver carcinoma, Hepatology 50 (2009) 1453–1463.
[20] B. Wang, D. Wei, V.E. Crum, E.L. Richardson, H.H. Xiong, Y. Luo, S. Huang, J.L. Abbruzzese, K. Xie, A novel model system for studying the double-edged roles of nitric oxide production in pancreatic cancer growth and metastasis, Oncogene 22 (2003) 1771.
[21] X. Qi, S.S. Lam, D. Liu, D.Y. Kim, L. Ma, L. Alleruzzo, W. Chen, T. Hode, C.J. Henry, J. Kaifi, E.T. Kimchi, G. Li, K.F. Staveley-O'Carroll, Development of inCVAX, in situ cancer vaccine, and its immune response in mice with hepatocellular cancer, J. Clin. Cell. Immunol. 7 (2016).
[22] G. Li, Y. Xu, D. Guan, Z. Liu, D.X. Liu, HSP70 protein promotes survival of C6 and U87 glioma cells by inhibition of ATF5 degradation, J. Biol. Chem. 286 (2011) 20251–20259.
[23] G. Li, D. Liu, E.T. Kimchi, J.T. Kaifi, X. Qi, Y. Manjunath, X. Liu, T. Deering, T. Fox, D.C. Rockey, T.D. Schell, M. Kester, K.F. Staveley-O'Carroll, Nanoliposome C6-ceramide increases the anti-tumor immune response and slows growth of liver tumors in mice, Gastroenterology 154 (4) (2018 Mar) 1024–1036.
[24] D. Liu, G. Li, D.M. Avella, E.T. Kimchi, J.T. Kaifi, M.P. Rubinstein, E.R. Camp, D.C. Rockey, T.D. Schell, K.F. Staveley-O'Carroll, Sunitinib represses regulatory T cells to overcome immunotolerance in a murine model of hepatocellular cancer, OncoImmunology 7 (2017) e1372079.
[25] D. Dluzen, G.F. Li, D. Tacelosky, M. Moreau, D.X. Liu, BCL-2 is a downstream target of ATF5 that mediates the prosurvival function of ATF5 in a cell type-dependent manner, J. Biol. Chem. 286 (2011) 7705–7713.
[26] D.M. Avella, G. Li, T.D. Schell, D. Liu, S.S.-M. Zhang, X. Lou, A. Berg, E.T. Kimchi, H.R.S. Tagaram, Q. Yang, S. Shereef, L.S. Garcia, M. Kester, H.C. Isom, C.B. Rountree, K.F. Staveley-O'Carroll, Regression of established hepatocellular carcinoma is induced by chemoimmunotherapy in an orthotopic murine model, Hepatology 55 (2012) 141–152.
[27] J. Kleeff, M. Korc, M. Apte, C. La Vecchia, C.D. Johnson, A.V. Biankin, R.E. Neale, M. Tempero, D.A. Tuveson, R.H. Hruban, J.P. Neoptolemos, Pancreatic cancer, Nat. Rev. Dis. Primers 2 (2016) 16022.
[28] J.F. Marshall, Targeting CDH17 in cancer: when blocking the ligand beats blocking the receptor? Clin. Cancer Res. 24 (2018) 253–255.
[29] R.A. Bartolome, C. Aizpurua, M. Jaen, S. Torres, E. Calvino, J.I. Imbaud, J.I. Casal, Monoclonal antibodies directed against cadherin RGD exhibit therapeutic activity against melanoma and colorectal cancer metastasis, Clin. Cancer Res. 24 (2018) 433–444.
[30] R.A. Bartolome, C. Aizpurua, M. Jaen, S. Torres, E. Calvino, J.I. Imbaud, J.I. Casal, Monoclonal antibodies directed against cadherin RGD exhibit therapeutic activity against melanoma and colorectal cancer metastasis, Clin. Cancer Res. 24 (2018) 433–444.
[31] H. Akl, T. Vervloessem, S. Kiviluoto, M. Bittremieux, J.B. Parys, H. De Smedt, G. Bultynck, A dual role for the anti-apoptotic Bcl-2 protein in cancer: mitochondria versus endoplasmic reticulum, Bba-Mol. Cell. Res. 1843 (2014) 2240–2252.
[32] S. Elmore, Apoptosis: a review of programmed cell death, Toxicol. Pathol. 35 (2007) 495–516.
[33] C.A. Stein, D. Castanotto, FDA-approved oligonucleotide therapies in 2017, Mol. Ther. 25 (2017) 1069–1075.

[34] M. Takamura, M. Sakamoto, Y. Ino, T. Shimamura, T. Ichida, H. Asakura, S. Hirohashi, Expression of liver-intestine cadherin and its possible interaction with galectin-3 in ductal adenocarcinoma of the pancreas, Cancer Sci. 94 (2003) 425–430.

[35] B.W. Wong, J.M. Luk, I.O. Ng, M.Y. Hu, K.D. Liu, S.T. Fan, Identification of liver-intestine cadherin in hepatocellular carcinoma–a potential disease marker, Biochem. Biophys. Res. Commun. 311 (2003) 618–624.

[36] X.Q. Wang, J.M. Luk, P.P. Leung, B.W. Wong, E.J. Stanbridge, S.T. Fan, Alternative mRNA splicing of liver intestine-cadherin in hepatocellular carcinoma, Clin. Cancer Res. 11 (2005) 483–489.

[37] B. Wang, D. Wei, V.E. Crum, E.L. Richardson, H.H. Xiong, Y. Luo, S. Huang, J.L. Abbruzzese, K. Xie, A novel model system for studying the double-edged roles of nitric oxide production in pancreatic cancer growth and metastasis, Oncogene 22 (2003) 1771–1782.